JOURNAL OF PROPULSION AND POWER
Vol. 13, No. 6, November–December 1997

Uncertainty Assessment of Ramjet Performance Determination in Connected-Pipe Testing

John A. Blevins* and Hugh W. Coleman†
University of Alabama in Huntsville, Huntsville, Alabama 35899

The results of an uncertainty assessment of data reduction methods for ramjet performance determination in connected-pipe testing are presented. The study reviews and investigates different methods of determining characteristic exhaust velocity *C, efficiency based on *C**, specific impulse *Isp*, efficiency based on *Isp*, and thermal efficiency. The uncertainty assessment of the data reduction methods is presented in two ways, one general and independent of test facility identity and one based on specific uncertainty estimates for input variables. The general case presents an uncertainty magnification factor illustrating how the uncertainty of each input variable is magnified or diminished as it propagates through the data reduction method into the result. The specific case presents an uncertainty percentage contribution of each input variable to the uncertainty of the result using specific uncertainty estimates for the input variables. It is shown that, for identical input variable values, the different data reduction methods give a wide range of performance values and uncertainties (a primary reason for the undertaking of this work). It is also shown that efficiencies based on *C** and *Isp* are poor parameters for characterizing ramjet combustion performance and are not recommended for use when comparing results that vary in altitude simulation.**

Introduction

CONNECTED-PIPE testing is used for performance determination and fundamental combustion studies in ramjet and scramjet engines.[1,2] A schematic of a typical connected-pipe facility is shown in Fig. 1. In such tests, the air supply is connected directly to the ramjet combustor and, therefore, connected-pipe testing considers only the combustor performance and no aerodynamic or inlet effects.

There exist various data reduction methods for each of the performance parameters associated with ramjet testing in connected-pipe facilities. An AGARD working group was tasked to review and report currently accepted methods for performance determination in connected-pipe testing. The subsequent report[3] issued by AGARD in 1994 presents the data reduction methods for performance determination that are currently used by the international technical community. For a given set of input variables, those data reduction methods yield a range of calculated values for each of the performance parameters (such as thermal efficiency, which ranged from 86 to 96% in the sample case presented in this paper for 16 different data reduction methods using identical inputs). The difference in the performance parameter values that can be determined by the use of the various data reduction methods using identical inputs is one of the motivating factors for the assessment of data reduction methods from an uncertainty analysis standpoint as presented in this paper.

The AGARD report used the uncertainty analysis approach[4] formulated by Abernethy et al.,[5–7] that has since been superseded by a more rigorous methodology internationally adopted in current guidelines and standards.[8–11] The analysis in this paper investigates the percentage contribution of the uncertainty of each variable to the uncertainty in the performance parameters, an aspect not discussed in the AGARD effort.[3]

The schematic of a connected-pipe facility shown in Fig. 1 includes station designation numbers that have been standardized[3] to simplify the reporting of test results. The station identification numbers are used as subscripts in this paper to denote the station. Station 2 corresponds to the postcompression inlet conditions, station 3 indicates upstream combustor conditions, station 4 indicates the combustor exit conditions, station 5 corresponds to the nozzle throat, and station 6 indicates the nozzle exit plane.

For the appropriate simulation of vehicle flight conditions, the air must be supplied at the stagnation temperatures and pressures that are to be encountered during flight. To supply the combustor with the high-temperature air necessary to simulate the conditions produced by a supersonic compression inlet, a vitiated heater is used to increase the air temperature. A vitiated heater uses combustion of a fuel added to the airflow to increase the temperature. Also, oxygen is added to the flowfield to offset the consumption of oxygen by the combustion of the vitiator fuel. By adding the fuel and makeup oxygen, the composition of the oxidizer supplied to the combustion chamber is no longer that of air because it includes combustion products from the vitiated heater. The composition can generally be considered to be all of the constituents (air, vitiator fuel, and makeup oxygen) at equilibrium at the static temperature and pressure of the inlets to the ramjet combustor.

The review and assessment of the data reduction methods presented in this paper include a description of the methods for selected performance parameters, a general uncertainty analysis for each of the data reduction methods, and a discussion of the appropriate use of the selected performance parameters.

Data Reduction Methodology

The various data reduction methods for selected performance parameters associated with ramjet testing in connected-pipe facilities are discussed in this section. These data reduction methods are those presented and discussed in the AGARD

Presented as Paper 95-3074 at the AIAA/ASME/SAE/ASEE 31st Joint Propulsion Conference, San Diego, CA, July 10–12, 1995; received Feb. 12, 1996; revision received July 24, 1997; accepted for publication July 24, 1997.

*Graduate Research Assistant, Propulsion Research Center, Department of Mechanical and Aerospace Engineering. E-mail: johnblevins@twlakes.net. Student Member AIAA.

†Eminent Scholar in Propulsion, Propulsion Research Center, Department of Mechanical and Aerospace Engineering. E-mail: coleman@ebs330.eb.uah.edu. Associate Fellow AIAA.

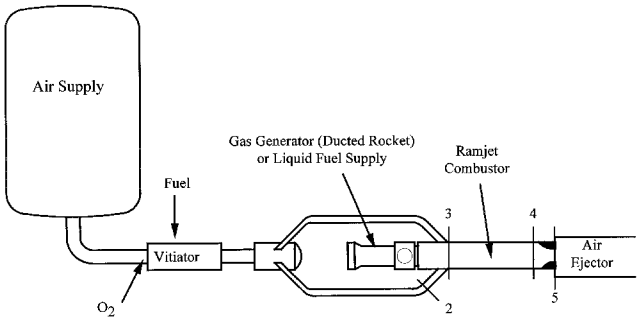

Fig. 1 Schematic of connected-pipe testing.

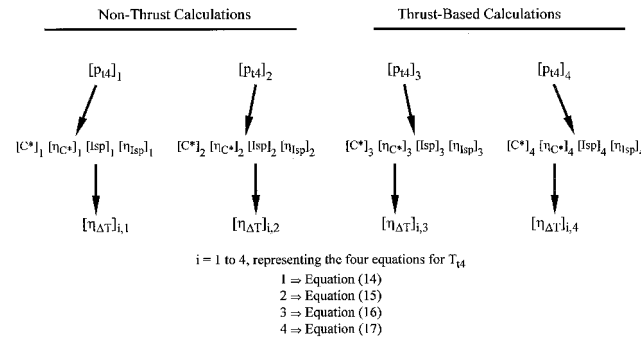

Fig. 2 Relationships among data reduction methods.

advisory report previously mentioned.[3] However, the presentation of the equations in this paper is different from the format of AGARD AR 323. In the AGARD report, the methods are presented as calculations with γ and without γ, referring to the direct use of the isentropic exponent γ. This led to the presentation of methods that are identical as separate methods in the AGARD report. In general, the methods designated as without γ use output that is computed by a chemical equilibrium combustion (CEC) code using an internally computed value of γ. In such instances, the determination of γ is transparent to the user (because it is internally computed by the CEC code), but is identical to the methods presented as with γ. Furthermore, the methods described as without γ are referred to as the more correct procedure.[3] The evaluation of these data reduction methods can only be justified by the use of appropriate uncertainty analysis techniques.

Chemical Equilibrium Combustion Codes

The majority of methods for performance determination utilize output from CEC codes. The codes, which were developed for classical rocket motor performance and species determination, are based on a zero-velocity combustion model because the Mach number in classical rocket motors is very small. To account for velocity in the combustion chamber of a ramjet, the accepted practice is to consider stagnation flow properties as inputs to the code instead of static flow properties.[3]

There are several different CEC codes in use. The two most frequently used codes are NASA CET89 (Refs. 12 and 13) and the JANNAF PEP code.[14] Previous investigations have shown no significant difference in the performance values calculated using the NASA CET89 and PEP codes.[3]

Performance Determination

Use of the different data reduction methods with identical inputs produces different calculated values for the performance parameters. The variation in these determined values using the same input parameters is one of the primary reasons for the undertaking of this study to assess the different methods of performance determination.

The performance parameters chosen as the subject of the uncertainty analysis assessment presented in this paper are characteristic exhaust velocity C^*, efficiency based on C^* (η_{C^*}), vacuum specific impulse Isp, efficiency based on Isp (η_{Isp}), and thermal efficiency ($\eta_{\Delta T}$). In this study, four distinct methods are identified for the determination of each of the parameters C^*, η_{C^*}, Isp, and η_{Isp}. The thermal efficiency $\eta_{\Delta T}$ can be determined from four different equations, two using C^* as input and two using Isp as input, resulting in 16 distinct data reduction methods for the determination of $\eta_{\Delta T}$.

In a slightly different approach to categorizing the methods than were used in the AGARD report, this study groups the data reduction methods for performance determination based on different methods for determining the total pressure at station 4 (p_{t4}). A diagram illustrating the relationship between p_{t4}, C^*, Isp, and $\eta_{\Delta T}$ is shown in Fig. 2.

The four methods for determining p_{t4} identified in this study are as follows.

Method 1:

$$p_{t4} = p_{t4\text{CEC}} \tag{1}$$

where $p_{t4\text{CEC}}$ is determined by a CEC code using the isentropic flow relations.

Method 2:

$$p_{t4} = p_4(1 + [(\gamma - 1)/2] \cdot M_4^2)^{\gamma/(\gamma-1)} \tag{2}$$

where p_4 is the measured static pressure at station 4, M_4 is the Mach number at station 4, and γ is the isentropic exponent that relates the properties of stations 4 and 5 as an isentropic process. The value of γ is obtained through the relation[3]

$$\gamma = \frac{\ell n(p_4/p_5)}{\ell n(p_4/p_5) - \ell n(T_4/T_5)} \tag{3}$$

where p_5, T_4, and T_5 can be found as output from the CEC codes.

The difference between methods 1 and 2 is that in method 1, the code uses an isentropic exponent that is not the same as γ used in method 2. The use of γ, as defined in Eq. (3), is the recommendation of the AGARD working group report because it exactly relates the properties of the end states (combustor exit and nozzle throat) by an isentropic process.

The process γ defined in the preceding text is not calculated directly by all codes. The value of the process γ lies within the range of values for the isentropic exponent based on frozen flow and the isentropic exponent based on equilibrium flow. For simplicity, in this paper, γ always refers to the process isentropic exponent based on the flow properties at stations 4 and 5, as defined in Eq. (3).

Method 3:

$$p_{t4} = \frac{F_5 + p_{\text{amb}}A_5}{(1 + \gamma CD_5)A_5}\left(\frac{\gamma + 1}{2}\right)^{\gamma/(\gamma-1)} \tag{4}$$

where p_{amb} is the ambient pressure, A_5 is the nozzle throat area (station 5), CD_5 is the nozzle discharge coefficient, and F_5 is the stream thrust as determined by

$$F_5 = F_{\text{LC}} - F_{\text{PL}} - A_b(p_b - p_{\text{amb}}) \tag{5}$$

where F_{LC} is the load cell measurement, F_{PL} is the preload on the load cell, A_b is the nozzle base area, and p_b is the base pressure.

Method 4:

$$p_{t4} = \left(\frac{C^*_{\text{th}}}{Isp_{\text{th}}}\right)\frac{F_5 + p_{\text{amb}}A_5}{CD_5A_5} \tag{6}$$

where C^*_{th} is the theoretical C^* calculated by the chemical equilibrium code, and Isp_{th} is determined by the code from

$$Isp_{\text{th}} = \frac{\dot{m}_5c_5 + p_5A_5}{\dot{m}_5} \tag{7}$$

where $\dot{m}_5$ is the mass flow rate at the nozzle throat, and c_5 is the velocity of exhaust gases at the nozzle throat. Assuming that the nozzle is choked, this corresponds to the speed of sound that is an output of the CEC codes.

The determination of C^* is based on the equation

$$C^* = p_{t4}A_5CD_5/\dot{m}_4 \tag{8}$$

where $\dot{m}_4$ is the total mass flow rate exiting the combustor and p_{t4} is from one of Eqs. (1), (2), (4), or (6), thus giving four ways to determine C^*.

The efficiency based on C^* is determined from

$$\eta_{C^*} = C^*/C^*_{\text{th}} \tag{9}$$

where C^* is determined from Eq. (8).

The determination of Isp is based on the equation

$$Isp = \frac{p_{t4}A_5}{\dot{m}_5}\left(\frac{2}{\gamma + 1}\right)^{\gamma/(\gamma-1)} \cdot (1 + \gamma CD_5) \tag{10}$$

where $\dot{m}_5$ is the mass flow rate at the nozzle throat (assuming that the mass flow in the combustor is expanded through the nozzle, $\dot{m}_5 = \dot{m}_4$), and p_{t4} is from one of Eqs. (1), (2), (4), or (6), thus giving four ways to determine Isp. Note that, when using Eq. (10) for determining the Isp based on the total pressure p_{t4}, determined by using Eq. (4), the influence of p_{t4} is eliminated, resulting in

$$Isp = \frac{F_5 + p_{\text{amb}}A_5}{\dot{m}_5} \tag{11}$$

The efficiency based on Isp is determined by

$$\eta_{Isp} = Isp/Isp_{\text{th}} \tag{12}$$

where Isp_{th} is the theoretical value for Isp determined by Eq. (7) and Isp is determined from Eqs. (10) or (11).

The determination of thermal efficiency is based on the equation

$$\eta_{\Delta T} = \frac{T_{t4,\text{exp}} - T_{t2}}{T_{t4,\text{th}} - T_{t2}} \tag{13}$$

where $T_{t4,\text{exp}}$, the total temperature at station 4, is calculated using experimental measurements and $T_{t4,\text{th}}$ is the theoretical total temperature at station 4 (adiabatic flame temperature based on stagnation flow properties) as determined by the use of a CEC code. Direct measurements to determine the cross-sectional average value of $T_{t4,\text{exp}}$ are generally not performed because of the difficulty in obtaining good results. For this reason, the direct measurement of $T_{t4,\text{exp}}$ is not considered in this paper. $T_{t4,\text{exp}}$ can be determined from four equations, two using C^* as inputs and two using Isp as inputs. Therefore, each equation for $T_{t4,\text{exp}}$ represents four different data reduction methods for $\eta_{\Delta T}$, as shown in Fig. 2. The equations for the determination of $T_{t4,\text{exp}}$ are

$$T_{t4,\text{exp}} = \gamma\left(\frac{2}{\gamma + 1}\right)^{(\gamma+1)/(\gamma-1)} \cdot \left(\frac{C^{*2}_{\text{exp}}}{R_4}\right) \tag{14}$$

$$T_{t4,\text{exp}} = \left(\frac{C^*_{\text{exp}}}{C^*_{\text{th}}}\right)^2 \cdot T_{t4,\text{th}} \tag{15}$$

$$T_{t4,\text{exp}} = \frac{\gamma}{2(\gamma + 1)} \cdot \left(\frac{Isp^2_{\text{exp}}}{R_4}\right) \tag{16}$$

$$T_{t4,\text{exp}} = \left(\frac{Isp_{\text{exp}}}{Isp_{\text{th}}}\right)^2 \cdot T_{t4,\text{th}} \tag{17}$$

where R_4 is the gas constant as determined by the use of a CEC code.

The diagram provided in Fig. 2 illustrates the relationships among the various data reduction methods. Each method for C^* and Isp corresponds to a method to determine p_{t4}. The methods for $\eta_{\Delta T}$ use the four different methods to determine p_{t4} in each of the four different equations for $T_{t4,\text{exp}}$ [Eqs. (14–17)], resulting in 16 methods for $\eta_{\Delta T}$. The subscripts shown in Fig. 2 for the performance determination methods are used throughout this paper and are provided for the identification of specific data reduction methods.

Uncertainty Analysis of Data Reduction Methods

To assess the uncertainty behavior associated with the different data reduction methods, an uncertainty analysis of a nominal case was performed. The nominal values for the case study used in this uncertainty analysis were taken from the case presented for example calculations in Ref. 3 and are presented in Table 1.

In this study, a general uncertainty analysis[15] was performed, and therefore, the uncertainties of the input variables are not considered separately in terms of bias and precision uncertainty components. Consider the uncertainty of a result r of a data reduction equation (DRE) with J input variables x_i, such that

$$r = r(x_1, x_2, \ldots, x_J) \tag{18}$$

The overall uncertainty in r can be determined by

$$\frac{U_r}{r} = \left[\sum_{i=1}^{J}\left(\frac{x_i}{r}\cdot\frac{\partial r}{\partial x_i}\right)^2\left(\frac{U_{x_i}}{x_i}\right)^2\right]^{1/2} \tag{19}$$

or equivalently, as

$$U_r = \left[\sum_{i=1}^{J}\left(\frac{\partial r}{\partial x_i}\right)^2 U^2_{x_i}\right]^{1/2} \tag{20}$$

where U_{x_i} is the uncertainty in the input variable x_i. The interval $r \pm U_r$ contains the true (but unknown) value of r about 95 times out of 100.

A general uncertainty analysis was performed considering the equations for C^*, η_{C^*}, Isp, η_{Isp}, and $\eta_{\Delta T}$ to be of the form of Eq. (18). The partial derivatives were numerically approximated by perturbing each input variable in sequence by 1% and determining the perturbed value of the result. This allowed determination of $\Delta r/\Delta x_i$ for each result and each input variable for the particular nominal values in this study. The PEP code was used to perform all CEC code runs.

The sensitivity of the uncertainty of the results to the uncertainties of the various measured input variables is presented in two ways, the uncertainty magnification factor (UMF) and the uncertainty percentage contribution (UPC).

The UMF is defined as

$$\text{UMF} = \frac{x_i}{r}\cdot\frac{\partial r}{\partial x_i} \tag{21}$$

and its significance can be seen by referring to Eq. (19). If the UMF is less than 1, this indicates that the influence of the uncertainty in the input variable diminishes as it is propagated through the DRE. If the UMF value is greater than 1, the influence of the uncertainty of the input variable is magnified as it propagates through the DRE (a 1% uncertainty in the input variable accounts for greater than 1% uncertainty in the final result). In this study, all UMF values are presented as positive numbers. The sign does not affect the overall uncertainty because all terms are squared in Eq. (19). The UMF is independent of the uncertainty estimates of the input variables and, therefore, provides an assessment of the sensitivity of the

Table 1 Values for liquid fuel ramjet case study

Input variable	Nominal value[a]	Uncertainty estimate
$\dot{m}_{air}$, kg/s	6.692	0.06
$\dot{m}_{fuel}$, kg/s	0.311	0.0016
p_4, Pa	568,800	6,900
p_2, Pa	650,200	6,900
p_{base}, Pa	78,065	1,000
p_{amb}, Pa	101,300	500
T_{t2}, K	606	5
H_{fuel}, kcal/kg	−482	50
A_4, m^2	0.022698	0.000136
A_5, m^2	0.012668	0.00010134
A_{base}, m^2	0.004304	0.00005814
CD_5	1.0	0.01
F_{LC}, N	13,400	67
F_{PL}, N	5,000	25

[a]Nominal values from sample case in AGARD AR323 (Ref. 3).

Table 2 UMF values for C^*

Input variables	Method 1	2	3	4
$\dot{m}_{air}$	0.95	0.94	0.95	0.68
$\dot{m}_{fuel}$	0.04	0.05	0.03	0.35
p_4	0.98	1.00	0.01	0.37
p_2	0.00	0.00	0.00	0.00
p_{base}	0.00	0.00	0.03	0.02
p_{amb}	0.00	0.00	0.18	0.18
T_{t2}	0.00	0.00	0.00	0.05
H_{fuel}	0.00	0.00	0.01	0.00
A_4	0.33	0.00	0.01	0.14
A_5	1.16	1.44	0.13	0.29
A_{base}	0.00	0.00	0.01	0.01
CD_5	1.00	1.00	0.45	1.00
F_{LC}	0.00	0.00	1.37	1.37
F_{PL}	0.00	0.00	0.51	0.51

Table 3 UMF values for h_{C^*}

Input variables	Method 1	2	3	4
$\dot{m}_{air}$	0.67	0.66	0.67	0.40
$\dot{m}_{fuel}$	0.57	0.58	0.56	0.18
p_4	0.96	0.98	0.01	0.39
p_2	0.00	0.00	0.00	0.00
p_{base}	0.02	0.02	0.05	0.04
p_{amb}	0.00	0.00	0.18	0.18
T_{t2}	0.10	0.10	0.10	0.06
H_{fuel}	0.00	0.00	0.01	0.00
A_4	0.34	0.02	0.01	0.12
A_5	1.16	1.44	0.13	0.29
A_{base}	0.00	0.00	0.01	0.01
CD_5	0.00	0.00	0.56	0.00
F_{LC}	0.00	0.00	1.37	1.37
F_{PL}	0.00	0.00	0.51	0.51

result to the input variables and data reduction methods that is independent of the measurement systems of specific test facilities. This type of analysis is most useful during the early planning stages of an experiment, as it serves to direct the experimenter to the input variables whose uncertainties may potentially influence the result uncertainty the most. The UMF values for the data reduction methods are presented in Tables 2–6.

The UPC is defined as

$$\text{UPC} = \left(\frac{\partial r}{\partial x_i} U_{x_i}\right)^2 \Bigg/ \sum_{i=1}^{J} \left(\frac{\partial r}{\partial x_i} U_{x_i}\right)^2 \times 100 \qquad (22)$$

Table 4 UMF values for *Isp*

Input variables	Method 1	2	3	4
$\dot{m}_{air}$	0.94	0.94	0.95	0.67
$\dot{m}_{fuel}$	0.05	0.06	0.04	0.34
p_4	0.97	0.99	0.00	0.38
p_2	0.00	0.00	0.00	0.00
p_{base}	0.01	0.01	0.03	0.02
p_{amb}	0.00	0.00	0.18	0.18
T_{t2}	0.00	0.00	0.00	0.04
H_{fuel}	0.01	0.01	0.00	0.00
A_4	0.33	0.01	0.00	0.13
A_5	1.16	1.44	0.13	0.29
A_{base}	0.00	0.00	0.01	0.01
CD_5	0.56	0.56	0.00	0.56
F_{LC}	0.00	0.00	1.37	1.37
F_{PL}	0.00	0.00	0.51	0.51

Table 5 UMF values for h_{Isp}

Input variables	Method 1	2	3	4
$\dot{m}_{air}$	0.39	0.39	0.40	0.12
$\dot{m}_{fuel}$	0.19	0.19	0.18	0.20
p_4	0.58	0.60	0.39	0.76
p_2	0.00	0.00	0.00	0.00
p_{base}	0.01	0.01	0.04	0.02
p_{amb}	0.00	0.00	0.18	0.18
T_{t2}	0.06	0.06	0.06	0.02
H_{fuel}	0.00	0.01	0.00	0.00
A_4	0.21	0.11	0.12	0.25
A_5	0.73	1.01	0.29	0.72
A_{base}	0.00	0.00	0.01	0.01
CD_5	0.56	0.56	0.00	0.56
F_{LC}	0.00	0.00	1.37	1.37
F_{PL}	0.00	0.00	0.51	0.51

and its significance can be seen by referring to Eq. (20). The UPC values show the percentage contribution of the squared uncertainty term for each variable to the squared uncertainty of the result for a particular situation, where values for the uncertainties for each variable (U_{x_i}) have been estimated. This type of analysis is most useful during the late planning and early design phases of an experiment. The UPC values used in this study are based on reasonable estimates for the overall uncertainty in the input variables for the case of a liquid fuel ramjet. The estimated uncertainties in the input variables are shown in Table 1.

A result uncertainty for each performance parameter is determined based on the uncertainty estimates used to determine the UPC values. The calculated result values, UPC values, and result uncertainties Ur for each method are presented in Tables 7–11. Figures 3–5 show a graphical summary of the nominal result values and uncertainties of η_{C^*}, η_{Isp}, and $\eta_{\Delta T}$ for the various data reduction methods. The uncertainties are presented in the form of uncertainty bands about the calculated values of the results.

Discussion of Results

The UMF values in Tables 2–6 show the potential influence of input variable uncertainties for each data reduction method prior to the assignment of uncertainty estimates for input variables. The UMF values for the nonthrust methods indicate that the influence of uncertainties in airflow rate, combustor static pressure, nozzle throat area, and discharge coefficient have the greatest potential influence on the result uncertainty. The UMF values for the thrust based methods generally indicate a reduction in the influence of the combustor static pressure measurement uncertainty replaced by a significant influence of thrust measurement uncertainties.

Table 6 UMF values for h_{DT}

Input variables	C^* methods								*Isp* methods							
	1, 1	1, 2	1, 3	1, 4	2, 1	2, 2	2, 3	2, 4	3, 1	3, 2	3, 3	3, 4	4, 1	4, 2	4, 3	4, 4
$\dot{m}_{air}$	1.99	1.99	1.99	1.16	2.01	2.01	2.01	1.17	1.99	1.99	1.99	1.16	1.17	1.16	1.17	0.35
$\dot{m}_{fuel}$	0.98	1.00	0.95	0.16	1.65	1.66	1.62	0.50	0.98	1.00	0.95	0.16	0.53	0.54	0.50	0.59
p_4	2.86	2.93	0.03	1.11	2.85	2.92	0.03	1.12	2.86	2.93	0.03	1.11	1.70	1.76	1.12	2.17
p_2	0.00	0.00	0.00	0.00	0.00	0.00	0.00	0.00	0.00	0.00	0.00	0.00	0.00	0.00	0.00	0.00
p_{base}	0.04	0.05	0.13	0.09	0.05	0.06	0.14	0.10	0.04	0.05	0.13	0.09	0.02	0.03	0.10	0.07
p_{amb}	0.00	0.00	0.52	0.51	0.00	0.00	0.52	0.51	0.00	0.00	0.52	0.51	0.00	0.00	0.51	0.50
T_{t2}	0.37	0.38	0.36	0.21	0.36	0.36	0.34	0.20	0.37	0.38	0.36	0.21	0.21	0.22	0.20	0.06
H_{fuel}	0.01	0.00	0.02	0.02	0.00	0.01	0.01	0.01	0.01	0.00	0.02	0.02	0.01	0.02	0.01	0.00
A_4	1.01	0.06	0.03	0.35	1.01	0.06	0.03	0.35	1.01	0.06	0.03	0.35	0.62	0.32	0.35	0.71
A_5	3.47	4.31	0.39	0.85	3.47	4.31	0.39	0.85	3.47	4.31	0.39	0.85	2.15	2.97	0.85	2.05
A_{base}	0.00	0.00	0.03	0.03	0.00	0.00	0.03	0.03	0.00	0.00	0.03	0.03	0.00	0.00	0.03	0.03
CD_5	2.95	2.95	1.31	2.89	0.00	0.00	1.65	0.00	1.64	1.65	0.00	1.61	1.62	1.62	0.00	1.59
F_{LC}	0.00	0.00	4.06	4.00	0.00	0.00	4.06	4.00	0.00	0.00	4.06	4.00	0.00	0.00	4.00	3.95
F_{PL}	0.00	0.00	1.50	1.48	0.00	0.00	1.50	1.48	0.00	0.00	1.50	1.48	0.00	0.00	1.48	1.46

Table 7 UPC values for C^*

Input variables	Method, C^*, m/s			
	1	2	3	4
	1112	1110	1119	1137
$\dot{m}_{air}$	17.9	15.9	49.1	16.7
$\dot{m}_{fuel}$	0.0	0.0	0.0	1.5
p_4	34.8	32.4	0.0	9.1
p_2	0.0	0.0	0.0	0.0
p_{base}	0.0	0.0	0.1	0.0
p_{amb}	0.0	0.0	0.5	0.3
T_{t2}	0.0	0.0	0.0	0.1
H_{fuel}	0.0	0.0	0.0	0.0
A_4	0.9	0.0	0.0	0.3
A_5	21.5	29.5	0.7	2.5
A_{base}	0.0	0.0	0.0	0.0
CD_5	24.8	22.2	13.5	45.3
F_{LC}	0.0	0.0	31.7	21.3
F_{PL}	0.0	0.0	4.4	3.0
Ur, %	2.0	2.1	1.2	1.5

Table 8 UPC values for h_{C^*}

Input variables	Method, η_{C^*}, %			
	1	2	3	4
	95.1	94.9	95.6	97.1
$\dot{m}_{air}$	13.2	11.1	27.4	13.1
$\dot{m}_{fuel}$	3.2	2.8	6.3	0.9
p_4	49.8	44.2	0.0	22.9
p_2	0.0	0.0	0.0	0.0
p_{base}	0.0	0.0	0.3	0.2
p_{amb}	0.0	0.0	0.6	0.8
T_{t2}	0.3	0.2	0.5	0.2
H_{fuel}	0.0	0.0	0.0	0.0
A_4	1.6	0.0	0.0	0.5
A_5	32.0	41.7	0.8	5.8
A_{base}	0.0	0.0	0.0	0.0
CD_5	0.0	0.0	23.7	0.0
F_{LC}	0.0	0.0	35.5	48.8
F_{PL}	0.0	0.0	4.9	6.8
Ur, %	1.6	1.8	1.1	1.0

Table 9 UPC values for *Isp*

Input variables	Method, *Isp*, Ns/kg			
	1	2	3	4
	1389	1387	1397	1419
$\dot{m}_{air}$	21.5	18.7	56.5	24.0
$\dot{m}_{fuel}$	0.0	0.0	0.0	2.0
p_4	41.8	38.1	0.0	13.7
p_2	0.0	0.0	0.0	0.0
p_{base}	0.0	0.0	0.2	0.1
p_{amb}	0.0	0.0	0.6	0.5
T_{t2}	0.0	0.0	0.0	0.1
H_{fuel}	0.0	0.0	0.0	0.0
A_4	1.2	0.0	0.0	0.4
A_5	26.2	35.1	0.9	3.7
A_{base}	0.0	0.0	0.0	0.0
CD_5	9.3	8.1	0.0	20.4
F_{LC}	0.0	0.0	36.8	30.9
F_{PL}	0.0	0.0	5.1	4.3
Ur, %	1.8	1.9	1.1	1.2

Table 10 UPC values for h_{Isp}

Input variables	Method, η_{Isp}, %			
	1	2	3	4
	96.6	96.4	97.1	98.7
$\dot{m}_{air}$	9.5	7.4	13.1	0.6
$\dot{m}_{fuel}$	0.7	0.6	0.9	0.5
p_4	38.0	32.5	22.9	41.0
p_2	0.0	0.0	0.0	0.0
p_{base}	0.0	0.0	0.2	0.0
p_{amb}	0.0	0.0	0.8	0.4
T_{t2}	0.2	0.2	0.2	0.0
H_{fuel}	0.0	0.0	0.0	0.0
A_4	1.3	0.3	0.5	1.1
A_5	26.5	40.1	5.8	15.9
A_{base}	0.0	0.0	0.0	0.0
CD_5	23.8	18.9	0.0	14.9
F_{LC}	0.0	0.0	48.8	22.6
F_{PL}	0.0	0.0	6.8	3.1
Ur, %	1.1	1.3	1.0	1.4

The UPC values and the result uncertainties provided in Tables 7–11 are based on the uncertainty estimates for the input variables as given in Table 1. Based on these uncertainty estimates, the combustor static pressure uncertainty and the nozzle throat area uncertainty generally dominate the result uncertainty for nonthrust performance determination methods. The thrust based methods tend to be most influenced by the airflow rate and thrust measurement uncertainties. For this case study, the uncertainty estimate of the thrust measurements was 0.5% of the measured value. Although the load cell uncertainty may be lower, this value is representative of a typical thrust measurement in an experimental setup. Lower uncertainties may be achieved by a calibration of the load cell as it exists in the facility. The result uncertainty values indicate that the thrust based methods generally have less uncertainty than the nonthrust methods, particularly for the thermal efficiency methods.

A graphical comparison of the UMF values and the UPC values for a thermal efficiency method is presented in Fig. 6. The UMF values indicate that the uncertainty in thermal effi-

Table 11 UPC values for $h_{\Delta T}$

	C^* methods, $\eta_{\Delta T}$, %								*Isp* methods, $\eta_{\Delta T}$, %							
Input variables	1, 1	1, 2	1, 3	1, 4	2, 1	2, 2	2, 3	2, 4	3, 1	3, 2	3, 3	3, 4	4, 1	4, 2	4, 3	4, 4
	86.4	85.9	87.8	91.9	86.4	85.9	87.8	92.0	86.4	85.9	87.8	91.9	90.6	90.0	92.0	96.3
$\dot{m}_{air}$	9.9	8.7	31.5	6.5	13.5	11.3	27.8	13.4	12.1	10.4	38.0	10.1	9.8	7.7	13.4	0.6
$\dot{m}_{fuel}$	0.8	0.7	2.4	0.0	3.0	2.6	5.9	0.8	1.0	0.9	2.9	0.1	0.7	0.6	0.8	0.5
p_4	37.2	34.3	0.0	11.1	49.7	44.0	0.0	22.6	45.7	41.0	0.0	17.1	38.0	32.4	22.6	40.7
p_2	0.0	0.0	0.0	0.0	0.0	0.0	0.0	0.0	0.0	0.0	0.0	0.0	0.0	0.0	0.0	0.0
p_{base}	0.0	0.0	0.3	0.1	0.0	0.0	0.3	0.2	0.0	0.0	0.3	0.1	0.0	0.0	0.2	0.0
p_{amb}	0.0	0.0	0.6	0.4	0.0	0.0	0.6	0.8	0.0	0.0	0.8	0.6	0.0	0.0	0.8	0.4
T_{t2}	0.3	0.3	0.8	0.2	0.4	0.3	0.7	0.3	0.4	0.3	1.0	0.3	0.3	0.2	0.3	0.0
H_{fuel}	0.0	0.0	0.0	0.0	0.0	0.0	0.0	0.0	0.0	0.0	0.0	0.0	0.0	0.0	0.0	0.0
A_4	1.1	0.0	0.0	0.3	1.5	0.0	0.0	0.5	1.4	0.0	0.0	0.4	1.2	0.3	0.5	1.1
A_5	23.8	32.3	0.9	2.8	32.0	41.7	0.8	5.7	29.2	38.6	1.1	4.4	26.6	40.2	5.7	15.8
A_{base}	0.0	0.0	0.0	0.0	0.0	0.0	0.0	0.0	0.0	0.0	0.0	0.0	0.0	0.0	0.0	0.0
CD_5	26.9	23.7	17.0	50.8	0.0	0.0	23.5	0.0	10.2	8.8	0.0	24.3	23.5	18.6	0.0	14.8
F_{LC}	0.0	0.0	40.8	24.4	0.0	0.0	35.5	49.0	0.0	0.0	49.2	37.6	0.0	0.0	49.0	22.9
F_{PL}	0.0	0.0	5.6	3.3	0.0	0.0	4.9	6.7	0.0	0.0	6.7	5.1	0.0	0.0	6.7	3.1
Ur, %	5.7	6.1	3.2	4.1	4.9	5.3	3.4	2.9	5.1	5.6	2.9	3.3	3.3	3.8	2.9	4.1

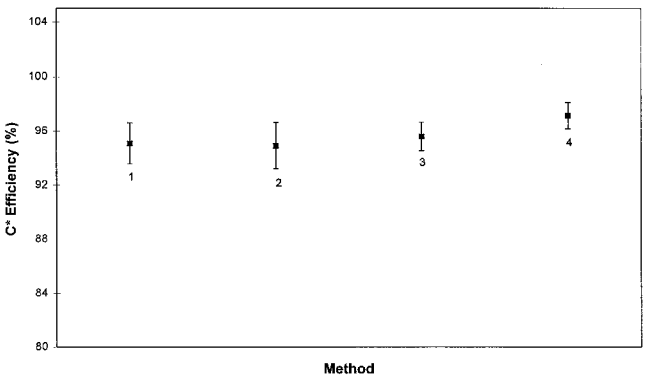

Fig. 3 Results for h_{C^*} methods.

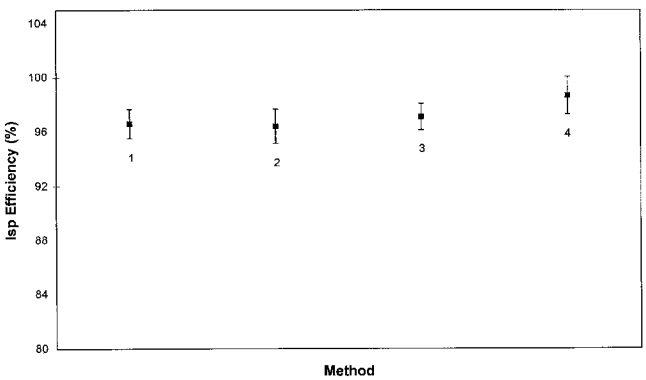

Fig. 4 Results for h_{Isp} methods.

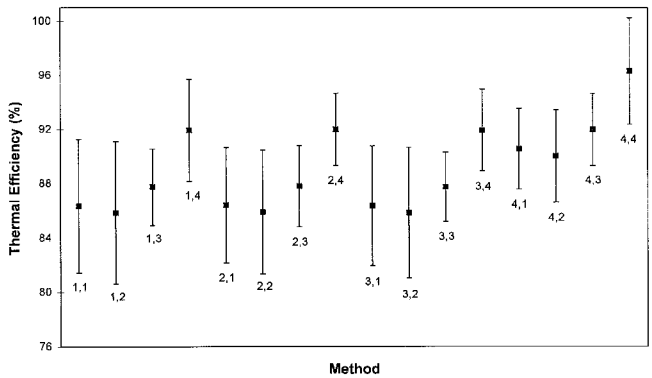

Fig. 5 Results for h_{DF}

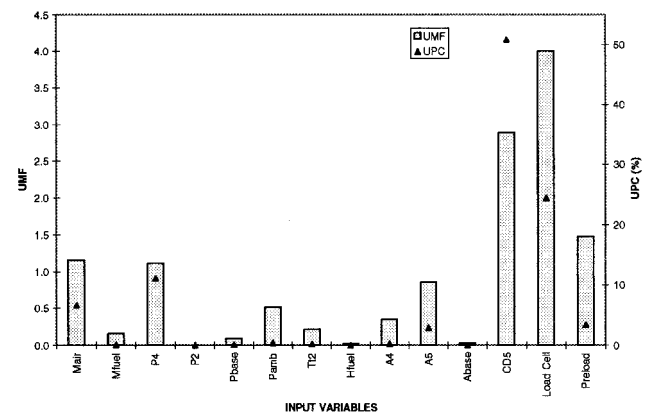

Fig. 6 UMF and UPC values for thermal efficiency method 1.4.

ciency is most sensitive to the load cell measurement. However, the UPC values show that, in fact, the discharge coefficient is the variable whose uncertainty most contributes to the result uncertainty once specific uncertainty estimates have been made for all variables. This illustrates the usefulness of the UPC values in targeting measurement uncertainties to improve the experimental result uncertainty to an acceptable value once uncertainty estimates for the input variables are made.

The result uncertainties presented in Tables 7–11 and shown graphically in Figs. 3–5 indicate that the methods for determining $\eta_{\Delta T}$ produce a larger range of values than do the methods for determining the other performance parameters and that the $\eta_{\Delta T}$ methods have the largest uncertainties of all of the performance parameters. In Fig. 5, it can be seen that all of the uncertainty bands do not overlap. This is probably because of the uncertainties associated with the assumptions in the methods, and these uncertainties were not considered in this study.

Note that the other efficiency performance parameters (η_{C^*} and η_{Isp}) are limited to a range of values that cannot approach zero because the airflow in the combustor always produces values of C^* and *Isp* that do not approach zero. Therefore, while the uncertainties of η_{C^*} and η_{Isp} in this study are lower than that of $\eta_{\Delta T}$, the resolution of possible values of η_{C^*} and η_{Isp} is less than that of possible values of $\eta_{\Delta T}$. This was observed in a recent study using a connected-pipe facility to compare proprietary ducted rocket propellants. In that study, a 2-km altitude simulation test that did not achieve ramjet combustion resulted in thermal efficiency values of less than 10% and values of η_{C^*} and η_{Isp} that were between 50 and 60%.

Furthermore, as the altitude simulation changes, the possible resolution of values for η_{C^*} and η_{Isp} varies. A 20 km simulation test that did not achieve ramjet combustion resulted in values of η_{C^*} and η_{Isp} that were around 80%.

This can be seen analytically by a review and discussion of the equation for η_{C^*}, which is given in Eq. (9), and reduces to

$$\eta_{C^*} = P_{t4}/P_{t4,\text{th}} \tag{23}$$

where $P_{t4,\text{th}}$ is the theoretical maximum total pressure attainable in the ramjet combustor. It can be seen by Eq. (23) that η_{C^*} is a pressure ratio term. Also, considering that both P_{t4} and $P_{t4,\text{th}}$ are functions of the total inlet pressure P_{t2}, that varies with altitude, η_{C^*} is a function of altitude. Similarly, η_{Isp} can be shown to also be a function of altitude. This leads to the conclusion that η_{C^*} and η_{Isp} are poor performance parameters for characterizing ramjet combustion because they are not valued from 0 to 100% and the resolution of values for η_{C^*} and η_{Isp} vary with altitude.

Summary and Conclusions

There exist numerous data reduction methods for the performance determination of ramjet connected-pipe testing. Analyzed in this study are four distinct methods for C^*, four distinct methods for *Isp*, and 16 distinct methods for thermal efficiency $\eta_{\Delta T}$. The uncertainty analysis study presented in this paper provides both a general and specific case assessment of the influence of input variable uncertainty on the result uncertainty for the various data reduction methods.

The UMF values illustrate the potential influence of the uncertainty of the measured variables to the result uncertainty prior to specific uncertainty estimates for the measured variables. This affords insight as to where to focus efforts at the beginning of the experiment planning phase.

Obtaining specific uncertainty estimates for the input variables allows the determination of the UPC values and result uncertainties. The UPC values show the influence of each variable uncertainty contribution squared to the result uncertainty squared in terms of percent. The usefulness of this analysis is that it shows which input variable uncertainties affect the result uncertainty the most. The UPC values based on the uncertainty estimates in this paper indicate that for the nonthrust calculations, the uncertainty in the static pressure measurement in the ramjet combustor and the uncertainty in nozzle throat area tend to influence the result uncertainty the most. For the thrust-based measurements, the result uncertainty is influenced most by the thrust, airflow rate, and discharge coefficient uncertainties.

The result uncertainty values allow direct comparison of data reduction methods based on the uncertainty estimates for the input variables. The uncertainty values determined show that the thrust-based methods typically provide results with lower values of uncertainty than the nonthrust calculations. This conclusion is particularly true for the $\eta_{\Delta T}$ values in Table 11. Furthermore, the thrust-based methods rely less heavily on the CEC code, and therefore, are influenced less than nonthrust calculations by the uncertainties that are associated with the CEC models (which are not considered in this study).

Finally, this study reviewed the choice of performance parameters in assessing ramjet combustion, and it is concluded that η_{C^*} and η_{Isp} are poor performance parameters for characterizing ramjet combustion because they are not valued from 0 to 100% and the resolution of values for η_{C^*} and η_{Isp} vary with altitude.

References

[1]Timnat, Y. M., "Recent Developments in Ramjets, Ducted Rockets and Scramjets," *Progress in Aerospace Sciences*, Vol. 27, 1990, pp. 201–235.

[2]Dunsworth, L. C., and Reed, G. J., "Ramjet Engine Testing and Simulation Techniques," *Journal of Spacecraft and Rockets*, Vol. 16, No. 6, 1979, pp. 382–388.

[3]"Experimental and Analytical Methods for the Determination of Connected-Pipe Ramjet and Ducted Rocket Internal Performance," AGARD Advisory Rept. 323, Aug. 1994.

[4]Vleghert, J. P. G., "Measurement Uncertainty Within the Uniform Engine Test Programme," AGARDograph No. 307, May 1989.

[5]Abernethy, R. B., Powell, B. D., Colbert, D. L., Sanders, D. G., and Thompson, J. W., *Handbook, Uncertainty in Gas Turbine Measurements*, Arnold Engineering Development Center, TR-73-5, Arnold Air Force Station, Feb. 1973.

[6]Abernethy, R. B., and Thompson, J. W., *Measurement Uncertainty Handbook*, Instrument Society of America, Revised, 1990.

[7]Abernethy, R. B., and Ringhiser, B., "History and Statistical Development of the New Measurement Uncertainty Methodology," ASME/SAE/AIAA/ISO Paper 85-1403, July 1985.

[8]*Guide to the Expression of Uncertainty in Measurement*, International Organization for Standardization, Geneve, Switzerland, 1993.

[9]*Quality Assessment for Wind Tunnel Testing*, AGARD-AR-304, 1994.

[10]*Assessment of Wind Tunnel Data Uncertainty*, AIAA Standard S-071-1995, AIAA, Washington, DC, 1995.

[11]Coleman, H. W., and Steel, W. G., "Engineering Application of Uncertainty Analysis," *AIAA Journal*, Vol. 33, No. 10, 1995, pp. 1888–1896.

[12]McBride, B. J., "Computer Program for Calculation of Complex Chemical Equilibrium Compositions, Rocket Performance, Incident and Reflected Shocks, and Chapman-Jouguet Detonations," NASA-SP-273, Revision July 1986.

[13]McBride, B. J., "CET89—Chemical Equilibrium with Transport Properties," NASA Lewis Research Center, Cleveland, OH, 1989.

[14]Cruise, D. R., "Theoretical Computations of Equilibrium Compositions, Thermodynamic Properties, and Performance Characteristics of Propellant Systems," Naval Weapons Center, TM-5164, China Lake, CA, April 1979.

[15]Coleman, H. W., and Steele, W. G., *Experimentation and Uncertainty Analysis for Engineers*, Wiley, New York, 1989.